

## Phosphoenolpyruvate-dependent Tubulin-Pyruvate Kinase Interaction at Different Organizational Levels\*

Received for publication, October 7, 2002

Published, JBC Papers in Press, December 13, 2002, DOI 10.1074/jbc.M210244200

János Kovács‡, Péter Löw‡, Anita Pác‡, István Horváth§, Judit Oláh§, and Judit Ovádi§¶

From the ‡Department of General Zoology, Eötvös Loránd University, P.O. Box 330, H-1445 Budapest, Hungary and the §Institute of Enzymology, Biological Research Center, Hungarian Academy of Sciences, P.O. Box 7, H-1518 Budapest, Hungary

**Evidence for the direct binding of pyruvate kinase to tubulin/microtubule and for the inhibitory effect of phosphoenolpyruvate on tubulin-enzyme hetero-association were provided by surface plasmon resonance and pelleting experiments. Electron microscopy revealed that pyruvate kinase induces depolymerization of paclitaxel-stabilized microtubules into large oligomeric aggregates and bundles of tubules in a salt concentration-dependent manner. The C-terminal “tail”-free microtubules did not bind pyruvate kinase, suggesting the crucial role of the C-terminal segments in the binding of kinase. Immunoblotting and polymerization experiments with cell-free brain extract revealed that pyruvate kinase specifically binds to microtubules, the binding of pyruvate kinase impedes microtubule assembly, and phosphoenolpyruvate counteracts the destabilization of microtubules induced by pyruvate kinase. We also showed by immunostaining the juxtannuclear localization of pyruvate kinase in intact L929 cells and that this localization was influenced by treatments with paclitaxel or vinblastine. These findings suggest that the distribution of the enzyme may be controlled by the microtubular network *in vivo*.**

Microtubules (MT)<sup>1</sup> constitute a crucial part of the cytoskeleton and are involved in a variety of cell functions such as maintenance of shape, organization of intracellular transport, motility, and cell division. The polymerization dynamics of MT is under strict control (1). In addition to small molecules (inorganic ions, guanine nucleotides, and drugs), numerous proteins are known to interact with MT as positive regulators of MT assembly (MAPs) either by promoting the polymerization of tubulin or by stabilizing MT (1, 2). Several other proteins including Op18/stathmin, katanin, and some kinesin-like proteins act as destabilizers (1, 2).

As shown by various methods including co-sedimentation assays and immunostaining, many glycolytic enzymes can interact transiently with the actin and/or microtubular network either *in vitro* or *in vivo*; the properties of associated partners (e.g. the stability of cytoskeleton and the activity of the enzyme)

are deeply influenced by the mutual interactions (Refs. 3–5; for review see Ref. 6). Recently, we found that two of the glycolytic enzymes, the M1 isoform of pyruvate kinase (PK) and *Dictyostelium discoideum* phosphofructokinase, can act as microtubule-destabilizing factors by inhibiting paclitaxel-induced polymerization of tubulin and by promoting disassembly of microtubules into thread-like oligomers (7, 8).

In the present study we have further characterized the PK-tubulin/MT interaction with purified proteins using surface plasmon resonance technology, and we present data on the heterologous association of PK with MTs in brain extract, the protein composition of which approximates that of the living cells. We present evidence on the crucial role of acidic C-terminal fragments of MTs in the PK binding. We show the modulating role of phosphoenolpyruvate (PEP) on tubulin-PK as well as on MT-PK interaction at different organization levels and demonstrate that the distribution of PK in mouse fibroblasts is highly dependent on the integrity of microtubular network.

### EXPERIMENTAL PROCEDURES

**Chemicals**—Rabbit muscle PK, ATP, EGTA, GDP, GTP, lactate dehydrogenase, MES, NADH, PEP, PK, phenylmethylsulfonyl fluoride, subtilisin, paclitaxel, and Tris were purchased from Sigma. Biotin-XX SSE (catalog no. B6352) was from Molecular Probes. All other chemicals were reagent grade commercial preparations. Solutions were prepared using Millipore's Milli-Q ultra-pure water.

**Protein Determination**—Protein concentration was measured by the Bradford method (9) using the Bio-Rad Protein Assay Kit. To determine the composition of pellets and supernatants in sedimentation experiments, proteins were separated on 9% SDS-PAGE. Stained gels as well as immunoblots were scanned using the Bio-Rad GelDoc 1000 densitometer system and quantitated using NIH Image software run on a Macintosh desktop computer.

**Tubulin and MT Preparation**—MAP-depleted tubulin was purified from bovine brain by the method of Na and Timasheff (10) and stored in 10 mM phosphate buffer, pH 7.0, containing 1 M sucrose, 0.5 mM MgCl<sub>2</sub>, and 0.1 mM GTP at –80 °C. Purified tubulin showed no contamination with MAPs on overloaded SDS-PAGE. Before use, stored tubulin was dialyzed against 50 mM MES buffer, pH 6.8, at 4 °C for 3 h and then centrifuged at 100,000 × *g* for 20 min at 4 °C. MT was assembled by adding 20 μM paclitaxel to 10 mg/ml tubulin, followed by incubation for 30 min at 37 °C.

**Enzyme Activity Assay**—The activity of PK was followed by monitoring the NADH consumption at 340 nm with a Cary 50 or a Jasco V-550 spectrophotometer utilizing a coupled enzymatic reaction with lactate dehydrogenase at 25 °C. The conditions for PK activity measurement corresponds to that described previously (7).

**Polymerization Assays**—10 μM tubulin was assembled to MT at 37 °C in 50 mM MES buffer, pH 6.6, containing 2 mM dithioerythritol, 5 mM MgCl<sub>2</sub>, 1 mM EGTA (polymerization buffer), and KCl in concentrations as indicated. The polymerization was initiated with 20 μM paclitaxel at 37 °C. PK was either incubated with tubulin for 20 min at 4 °C before starting the polymerization or added to the paclitaxel-stabilized MTs. For turbidity measurements, absorbance was monitored at 350 nm with a Cary 50 spectrophotometer. The error rate of determinations of tur-

\* This work was supported by grants from the Hungarian National Scientific Research Foundation, OTKA (T 029910 to J. K. and T 031892 to J. O.), and from the Hungarian Ministry of Education (NKFP-1-047/2001 MediChem to J. O.). The costs of publication of this article were defrayed in part by the payment of page charges. This article must therefore be hereby marked “advertisement” in accordance with 18 U.S.C. Section 1734 solely to indicate this fact.

¶ To whom correspondence should be addressed. Tel.: (36-1) 279-3129; Fax: (36-1) 466-5465; E-mail: ovadi@enzim.hu.

<sup>1</sup> The abbreviations used are: MT, microtubule; MAP, microtubule associated protein; MES, 2-(*N*-morpholino)ethanesulfonic acid; PEP, phosphoenolpyruvate; PK, pyruvate kinase; RU, resonance unit.

bidity measurements was  $\pm 5\%$  within a series of experiments, *i.e.* using the same tubulin stock solution and polymerizing buffer or the same freshly prepared cell-free extract. In another set of experiments the absolute value of the rate of turbidity increase could be different; however, the relative inhibitory effect caused by PK was within  $\pm 5\%$  error. The standard error of fitting of the polymerization curves for determination of the rates was  $\pm 2\%$ .

**Limited Proteolysis of MT**—The acidic C-terminal fragments of paclitaxel-stabilized MTs were selectively removed by limited subtilisin digestion as described by Wang and Sheetz (11), and the product was analyzed by SDS-PAGE, which provided evidence for the cleavage of the fragments from both tubulin subunits.

**Pelleting Experiments**—MAP-free tubulin or subtilisin-treated MTs at final concentrations of  $10 \mu\text{M}$  were incubated with or without  $2 \mu\text{M}$  PK in polymerizing buffer for 30 min at  $37^\circ\text{C}$ . The samples were centrifuged at  $100,000 \times g$  for 20 min at  $30^\circ\text{C}$ . Under these conditions MTs and MT-bound PK are completely pelleted, whereas uncomplexed PK remains in the supernatant (7). The partition of the proteins into pellet and supernatant fractions was analyzed by SDS-PAGE separation in 9% polyacrylamide gels. To study the influence of PEP on the partition of PK, a set of pelleting experiments was performed in the presence of  $100 \mu\text{M}$  PEP.

**Preparation of Cell-free Cytosolic Fraction**—Cell-free cytosolic fraction containing the soluble proteins of cells including tubulin and MAPs ( $30 \text{ mg/ml}$  total protein concentration) was prepared from bovine brain as described previously (12). To initiate MT formation, the fraction was warmed to  $37^\circ\text{C}$  in the presence of  $1 \text{ mM}$  GTP and  $20 \mu\text{M}$  paclitaxel.

**Immunoblot of PK**—Serum against rabbit muscle PK was raised by immunizing rats as described previously (7). The IgG fraction was purified according to Tracey *et al.* (13). Proteins from the brain cell-free extract and from the pellet and supernatant fractions of the co-sedimentation experiments were separated on SDS-PAGE and transferred to nitrocellulose membranes. The anti-PK IgG was used at a 500-fold dilution from a  $20 \text{ mg/ml}$  stock solution. The secondary antibody-alkaline phosphatase conjugate (Sigma) was used at a dilution of 1:5000. The immunocomplex was visualized by the 5-bromo-4-chloro-3-indolyl phosphate/nitro blue tetrazolium (BCIP/NBT) chromogenic detection system.

**Cell Culture**—L929 cells were plated on glass coverslips and maintained in Dulbecco's modified Eagle's medium containing 10% fetal calf serum. For testing the effect of anti-microtubular drugs, the cells were incubated for 2 h in the presence of  $10 \mu\text{g/ml}$  paclitaxel or  $1 \mu\text{g/ml}$  vinblastine. For immunostaining, the cells were fixed in cold methanol. PK-antiserum, prepared as described above, was used to label PK at 1:50 dilution followed by fluorescein isothiocyanate-conjugated anti-rat IgG (Sigma) to visualize the immunocomplex under a fluorescent microscope.

**Transmission Electron Microscopy**—MT-containing samples were pelleted by centrifugation, and the pellets were pre-fixed with 2% glutaraldehyde, 0.2% tannic acid in  $0.1 \text{ M}$  sodium cacodylate, pH 7.4, for 60 min and then washed with  $0.1 \text{ M}$  sodium cacodylate, post-fixed with  $0.5\%$   $\text{OsO}_4$  in  $0.1 \text{ M}$  sodium cacodylate, stained *en bloc* with 1% uranyl acetate, dehydrated in graded ethanol, and embedded in Durcupan (Fluka). Thin sections, contrasted with uranyl acetate and lead citrate, were examined and photographed in a JEOL CX 100 electron microscope.

**Surface Plasmon Resonance (SPR)**—The binding kinetics of PK to tubulin was monitored in real-time with a BIAcore X instrument (BIAcore AB, Uppsala, Sweden). Tubulin at a concentration of  $10 \text{ mg/ml}$  was biotinylated with a sulfosuccinimidyl ester derivative of biotin, and the biotinylated tubulin at a concentration of  $0.5 \mu\text{M}$  was immobilized onto a streptavidin-coated sensor chip (Sensor Chip SA, product code BR-1000-32, BIAcore) as described previously (12). All experiments were performed at  $25^\circ\text{C}$ . Sensorgrams were recorded at a flow rate of  $5 \mu\text{l/min}$  for 3 min at different concentrations of PK in the absence and presence of PEP. In some cases the injected sample contained  $100 \text{ mM}$  KCl in addition to PK. Dissociation and association rate constants were calculated using the Langmuir (1:1) binding model by the BIAevaluation 3.0 software supplied by the manufacturer or by the linearization methods based upon Equation 1 (14),

$$\ln \frac{dR}{dt} = \ln(k_{\text{on}}CR_{\text{max}}) - (k_{\text{on}}C + k_{\text{off}})t \quad (\text{Eq. 1})$$

where  $R$  is the resonance signal in RU at time  $t$ ,  $dR/dt$  is the rate of change of the SPR signal,  $C$  is the concentration of the analyte (PK), and  $R_{\text{max}}$  is the maximum analyte binding capacity in RU. The slope of the plot of  $\ln(dR/dt)$  versus  $t$  is  $-(k_{\text{on}}C + k_{\text{off}})$ , which we designated  $k_{\text{obs}}$ , and

the tangent of  $k_{\text{obs}}$  versus  $C$  gives  $k_{\text{on}}$  (the knowledge of  $R_{\text{max}}$  is not necessary). For linear fitting we used Microcal Origin version 5.0 software (Microcal Software Inc.). The error of determination was  $\pm 10\%$ .

## RESULTS

**Quantitative Characterization of PK-Tubulin Interaction and the Effect of PEP on the Interaction**—To obtain direct quantitative data on the binding of PK to tubulin, the association and dissociation kinetics of the interaction were followed by surface plasmon resonance measurements. Fig. 1A shows typical sensorgrams obtained at 65, 86, 108, and  $129 \text{ nM}$  PK concentrations. The kinetic constants obtained by nonlinear fitting are:  $k_{\text{on}} = 2.44 \times 10^5 \text{ M}^{-1}\text{s}^{-1}$ ;  $k_{\text{off}} = 1.02 \times 10^{-2} \text{ s}^{-1}$ . The dissociation constant,  $K_d = k_{\text{off}}/k_{\text{on}}$ , is  $4.18 \times 10^{-8} \text{ M}$ . The  $k_{\text{on}}$  value was also calculated from the slope of  $k_{\text{obs}}$  versus  $C$  (Fig. 1C) as described under "Experimental Procedures." The value of  $k_{\text{on}}$  is  $(1.94 \times 10^5 \pm 2.9 \times 10^3) \text{ M}^{-1}\text{s}^{-1}$ , which is in good agreement with the value obtained from nonlinear direct fitting of SPR sensorgrams. In the presence of  $100 \text{ mM}$  KCl, virtually no PK binding could be detected (data not shown).

To study the effect of PEP on tubulin-PK interaction, a solution of  $65 \text{ nM}$  PK containing different concentrations of PEP was injected over the tubulin-coated surface. The rate constant of the dissociation process evaluated from the sensorgrams obtained at various PEP concentrations is independent of the PEP concentration (data not shown), however, the  $\text{RU}_{\text{equ}}$  values, which are characteristic for the amount of PK bound to tubulin, decreased with increasing PEP concentrations (see Fig. 1D). These data suggest that PEP competes with tubulin for PK binding.

**PK Targets Negatively Charged C-terminal "Tails" on MTs**—Previously we demonstrated by differential centrifugation that PK induces the formation of less sedimentable tubulin oligomers and binds preferentially and stoichiometrically to this tubulin oligomer fraction (7). The finding that the kinase is present in the high speed pellet ( $100,000 \times g$ ) provided evidence for its binding to the tubulin oligomer/MT. Here we have investigated the effect of ionic strength on the binding of PK to MTs.  $2 \mu\text{M}$  PK was added to paclitaxel-stabilized MTs in the presence of either  $50$  or  $150 \text{ mM}$  KCl in the polymerizing buffer, and then the samples were centrifuged at  $100,000 \times g$ , and the pellets were analyzed by transmission electron microscopy. Long smooth-surfaced intact MTs are seen in the control samples (Fig. 2A). When PK was added to these MTs at low ionic strength, the samples became crowded with large thread-like aggregates. Among these aggregates, bundled MTs arranged in parallel and connected by rows of small dense particles could be observed (Fig. 2B). Bundled MTs and the aggregates were practically absent in samples prepared at high ionic strength (Fig. 2D), which is in agreement with our SPR data obtained with unpolymerized tubulin, showing that high salt concentration inhibits the complex formation of tubulin with PK.

The aggregates and bundled MTs were also conspicuous in samples containing PK and  $1 \text{ mM}$  pyruvate at low salt concentration (data not shown). By contrast, if the sample contained  $1 \text{ mM}$  PEP instead of pyruvate, the amount of both bundled MTs and thread-like aggregates was greatly reduced (Fig. 2C). The effect of PEP on the association of PK to MTs was demonstrated by pelleting experiments as well. As shown in Fig. 3A, after centrifugation of samples containing MT + PK practically all MT appeared in the pellet together with significant amounts of PK. The addition of  $1 \text{ mM}$  PEP reduced the amount of PK co-sedimented with MTs. These observations indicate that PEP specifically inhibits the association of PK to MTs.

To study the role of the acidic C-terminal tail of tubulin exposed on the surface of MTs in the salt-sensitive binding of PK, the pelleting experiments were also performed with "tail-

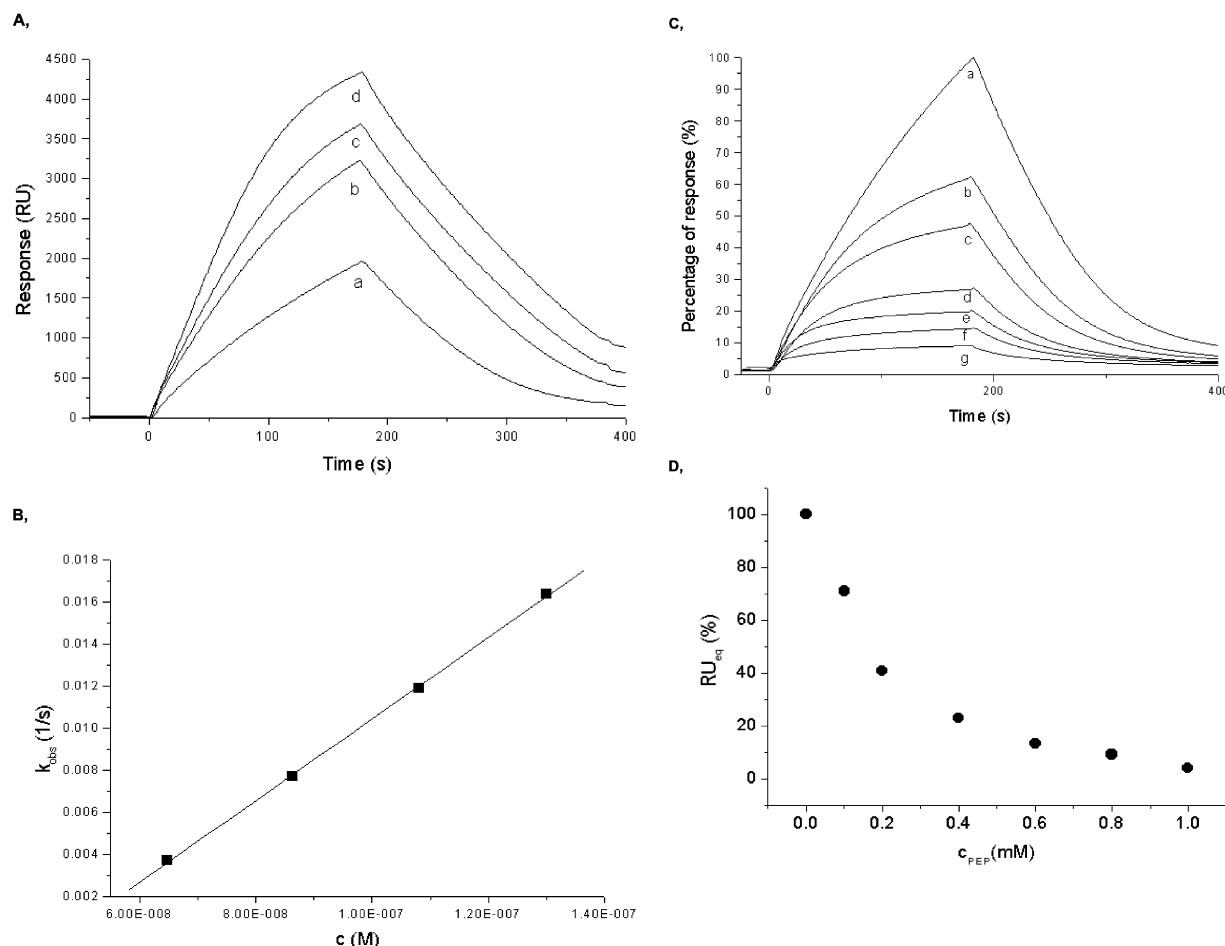


**FIG. 1. PK-tubulin interaction monitored by surface plasmon resonance and the effect of PEP.** Sensorgrams of injections of PK alone (A: 65 nM (a), 86 nM (b), 108 nM (c), and 129 nM (d)) and 65 nM PK in the presence of various PEP concentrations (C: 0 mM (a), 0.1 mM (b), 0.2 mM (c), 0.4 mM (d), 0.6 mM (e), 0.8 mM (f), and 1 mM (g)). B, determination of  $k_{on}$  by straight line fitting of the  $k_{obs}$  versus  $C$  (PK concentration) graph. D, dependence of  $RU_{eq}$  values on PEP concentrations.

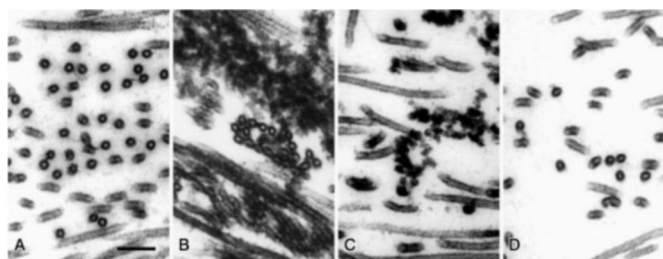


**FIG. 2. Electron microscopy of PK-MT interaction.** Microtubules assembled as described under "Experimental Procedures" were incubated without (A) or with the addition of PK (B and D) or PK + PEP (C) in the presence of 50 mM KCl (B and C) or 150 mM KCl (D). Note the thread-like aggregates and bundled MTs in B. Their presence is less conspicuous in C, and they are absent in A and D. Bar, 125 nm.

free" MT prepared by limited subtilisin digestion as suggested by Wang and Sheetz (11). The release of the C-terminal tails of tubulin subunits was monitored by SDS-PAGE, and as shown in Fig 3B, after a 60-min digestion the limited proteolysis was completed. When PK was added to the tail-free MTs under the conditions used for intact MTs, and the pellet fractions were analyzed, no PK was detected in the pellet fraction. Examination of the subtilisin-digested MTs by transmission electron microscopy revealed that the tail-free MTs are significantly shorter than their intact counterparts in accordance with the observation of Wang and Sheetz (11), and neither the oligomerization nor the bundling of MTs could be observed in the PK-containing samples prepared even at low salt concentration

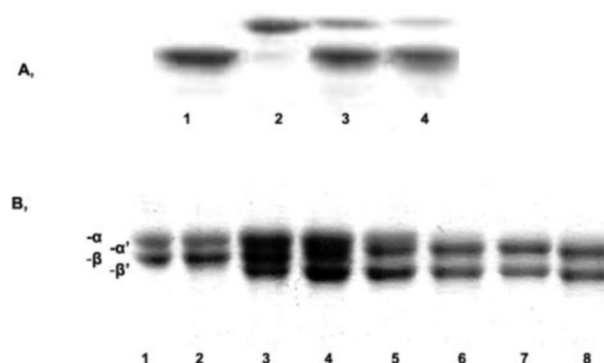


**FIG. 3. Pelleting experiments with paclitaxel-stabilized intact (A) and tail-free (B) MTs.** Conditions for MT assembly induced by paclitaxel and for the pelleting experiments are described under "Experimental Procedures." A, SDS-PAGE images of pellets (MT alone (lane 1), MT + PK (lane 3), MT + PK + PEP (lane 4)) and of supernatant (PK alone (lane 2)). B, time dependence of MT digestion by subtilisin (cf. "Experimental Procedures") at: 0 min (lane 2), 2 min (lane 3), 10 min (lane 5), 30 min (lane 6), and 60 min (lane 7). Lane 1, control (no subtilisin added); lane 8, tail-free MT + PK.

(data not shown). These data are in contrast to those obtained with intact MTs (cf. Fig. 3A) and reveal the crucial role of the negatively charged C-terminal tails of MT in the PK-MT interaction.

*Characterization of PK-MT Interaction in Brain Cell-free Extract*—The experiments with purified proteins described



TABLE I  
Effect of MT assembly on the distribution of PK in brain cell-free extract

Brain cell-free extract (30 mg/ml total protein concentration) was warmed to 37 °C, and MT formation was initiated by adding 1 mM GTP and 20  $\mu$ M paclitaxel. After centrifugation at 100,000  $\times$  *g*, the amount of PK in the pellet and supernatant was analyzed by activity measurements and densitometry of immunoblots as described under "Experimental Procedures." The data are the average of at least three independent measurements. Relative error of determinations is less than 10%.

Sample	Activity measurements				Immunoblotting	
	Control		GTP + paclitaxel		Control	GTP + paclitaxel
	units/ml	%	units/ml	%	%	%
Extract	54.1	100	54.1	100	100	100
Supernatant	51.6	95	43.3	80	>95	75
Pellet	2.5	5	10.8	20	<5	19

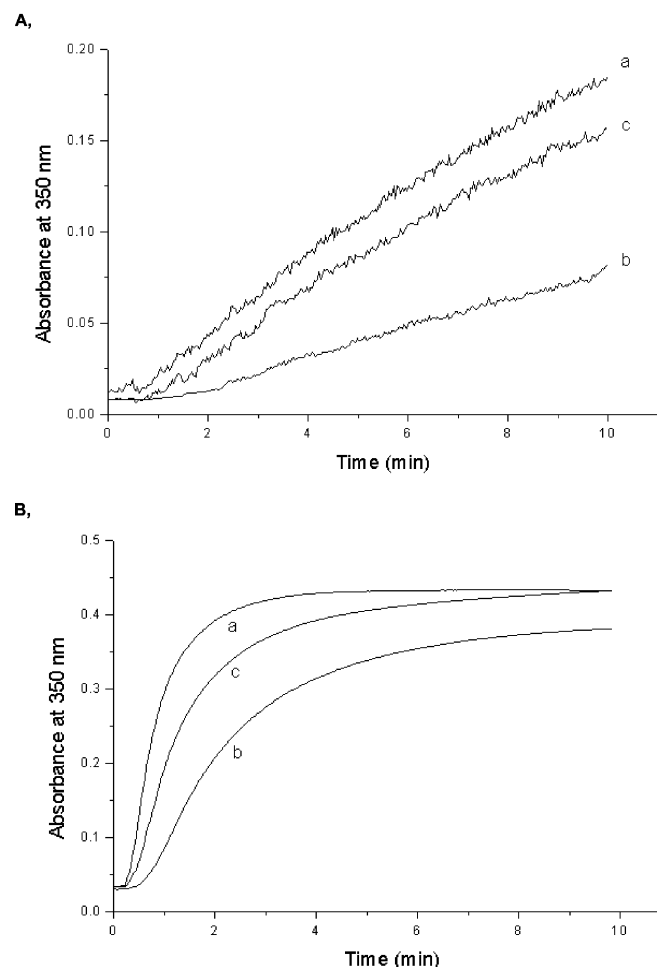


FIG. 4. Polymerization of endogenous tubulin in brain extract (A) and in a solution of purified tubulin (B) in the absence (a) or presence of PK (b) and PK + PEP (c). The concentrations of PEP, PK, and tubulin in B are 100, 2, and 10  $\mu$ M, respectively.

above clearly show that both tubulin and MT bind PK and the binding occurs at relatively low protein concentrations. To obtain direct evidence for the occurrence of this hetero-association in a complex system, the interaction of PK with tubulin/MT was investigated in brain extract, which mimics the cellular conditions concerning the composition of soluble proteins. In one set of experiments the co-pelleting of endogenous PK with MTs formed by paclitaxel-induced polymerization was tested by analyzing the partition of PK in the supernatant and the pellet fractions in the absence and presence of assembled MTs. The MT assembly was induced by adding GTP plus paclitaxel to the concentrated cell-free extract (30 mg/ml), and the pellet and supernatant fractions were analyzed for the partition of PK by activity measurements as well as by immunoblotting using anti-PK antibody. As shown in Table I, both methods

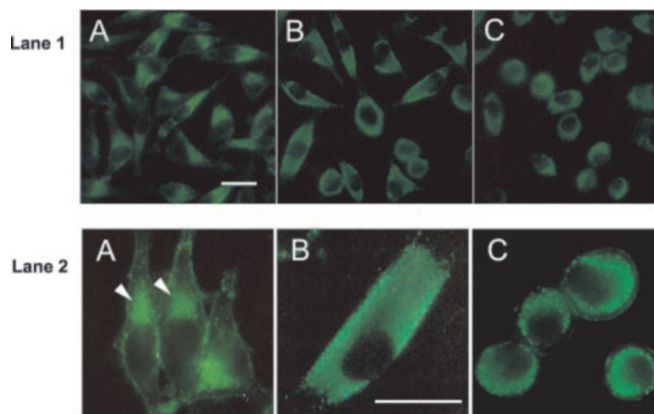


FIG. 5. Immunohistochemistry of PK in intact L929 cells (A) and following treatment with paclitaxel (B) or vinblastine (C). The PK is concentrated in a domain near the nucleus, as indicated by arrowheads in the control cells. Lanes 1 and 2 are the low power and high power magnifications, respectively. Bar, 100  $\mu$ m

revealed that about 20% of the endogenous PK co-sedimented with the MTs. It has to be noted that less than 5% of the extract proteins, including endogenous PK, appeared in the pellet prepared without the addition of GTP + paclitaxel.

In another set of experiments, MT assembly in brain extract was also initiated by adding paclitaxel and followed by turbidimetry in the absence and presence of exogenous PK or PK plus PEP added to the extract prior to starting the polymerization of endogenous tubulin. As shown in Fig. 4A, PK decreases the rate of polymerization. However, the simultaneous addition of PEP with exogenous PK partially suspends this effect. Fig. 4B shows the counteracting effect of PEP on PK-induced inhibition of tubulin polymerization with purified proteins as well. These data reveal that PK and MT can mutually recognize and interact with each other not only in purified systems but in extract containing a number of other microtubular (e.g. MAPs) and cytosolic proteins, which suggests the binding of PK to microtubular apparatus in complex biological systems.

**Localization of PK in L929 Cells**—Previously we demonstrated the localization of PK on tubulin polymers by immunoelectron microscopy in an *in vitro* system using anti-PK immunogold labeling (7). Here we aimed to visualize the distribution of PK, known as cytosolic enzyme, in living cells. The distribution of the enzyme was studied by immunohistochemical method in L929 cells. As shown in Fig. 5A, although the intact L929 cells have an elongated shape, PK as shown by the bright fluorescence is concentrated in a juxtannuclear part of their cytoplasm. The nucleus and the extensions of the cells are not stained.

To obtain information about the role of the microtubular network in the localization of PK, cells treated with the anti-microtubular drugs paclitaxel or vinblastine were also studied. The paclitaxel-treated cells maintained the elongated shape

characteristic of intact L929 cells, showing, however, an altered staining pattern in most cells (Fig. 5B). Although cells similar to the untreated cells are found because of the inhomogeneity of the cells, however, the major fraction of these cells behaved differently than the control cells; the distinct juxtannuclear concentration of the stain was no longer visible, and instead diffuse staining over extended areas of cytoplasm could be observed (Fig. 5B). The difference in PK localization is more evident in the colored images with high power magnification.

The shape of the vinblastine-treated cells was changed dramatically because of the collapse of the microtubular network, and the round cells showed an unlocalized distribution of the fluorescently labeled PK (Fig. 5C). Although colocalization of PK and individual MTs was not examined in these experiments, our observations show that the intracellular localization of the kinase is strongly influenced by the organization of the MT network.

#### DISCUSSION

Our data demonstrate that both the polymerized and unpolymerized tubulin interacts with PK. SPR technique was used here for the first time to characterize the kinetic and affinity parameters of this interaction. The high affinity of PK to tubulin, characterized by a low dissociation constant, made it possible to use low protein concentrations in the experiments with purified proteins for association studies and to detect this hetero-association in cell-free extract. As shown by electron microscopy, the bundling of MTs and the appearance of thread-like oligomeric aggregates are the morphologic manifestations of this interaction. Both processes were suppressed under high salt conditions and were absent in subtilisin-treated MT samples. These data are in good agreement with earlier observations demonstrating the sensitivity of PK-tubulin interaction to salt concentration (15) and to proteolytic cleavage of the C-terminal segment of tubulin (16). The mechanism of formation of oligomeric aggregates needs further elucidation. These aggregates accumulated in the presence of PK in samples during paclitaxel-induced tubulin polymerization as well as in samples of preassembled paclitaxel-stabilized MTs, which are practically free of nonsedimenting tubulin dimers. This suggests that the enzyme induces partial depolymerization of MTs. The presence of PK in the oligomeric aggregates was demonstrated earlier by SDS-PAGE analysis as well as by immunocytochemistry (7). It is tempting to speculate that occupation of the C-terminal tails of tubulins by PK may weaken the contacts necessary for the ordered arrangement of tubulin dimers in the cylindrical wall of MTs but do not suppress their propensity to

bind each other and form atypical tubulin assemblies as observed in our experiments.

An important finding of our study is that PEP can suppress the binding of PK to tubulin/MTs. This effect was demonstrated by four independent methods, SPR, pelleting, electron microscopy, and turbidimetry, in a system containing pure proteins only and in brain extracts as well. PK is a key glycolytic enzyme, present in the brain in micromolar concentrations (17), which is within the range used in our experiments. Our data suggest that in living cells a significant fraction of the PK could be in an associated form around the nucleus. The localization of PK could be the result of the hetero-association of the kinase in which the microtubular network might be involved. The organization of the microtubular network is an important issue in the formation of macromolecular superstructure, as indicated by the results obtained using various drug treatments. Under physiological conditions, however, the PEP could modulate the distribution of PK within the cytoplasm. The binding is counteracted by PEP, a crucial intermediary in glycolysis, the concentration of which is controlled by the metabolic state of the cells.

*Acknowledgments*—The skillful assistance of Sarolta Sipos and Emma Hlavanda is gratefully acknowledged. We thank Zsolt Pálfi for help with the layout of microscopic figures. We thank Dr. Angelica Keller for critical reading of the manuscript and Dr. Ferenc Orosz for helpful discussions.

#### REFERENCES

- Desai, A., and Mitchinson, T. J. (1997) *Annu. Rev. Cell Dev. Biol.* **13**, 83–117
- Nogales, E. (2000) *Annu. Rev. Biochem.* **69**, 277–302
- Wojtas, K., Slepecky, N., von Kalm, L., and Sullivan, D. (1997) *Mol. Biol. Cell.* **8**, 1665–1675
- Srere, P. A., and Knull, H. R. (1998) *Trends Biochem. Sci.* **23**, 319–320
- Wagner, G., Kovács, J., Löw, P., Orosz, F., and Ovádi, J. (2001) *FEBS Lett.* **509**, 81–84
- Ovádi, J., and Orosz, F. (1996) in *Channeling in Intermediary Metabolism* (Agius, L., and Sherratt, H. S. A., eds) pp. 237–268, Portland Press, London
- Vértessy, B. G., Bánkfalvi, D., Kovács, J., Löw, P., Lehotzky A., and Ovádi, J. (1999) *Biochem. Biophys. Res. Commun.* **254**, 430–435
- Orosz, F., Santamaria, B., Ovádi, J., and Aragon, J. J. (1999) *Biochemistry* **38**, 1857–1865
- Bradford, M. M. (1976) *Anal. Biochem.* **72**, 248–254
- Na, G. C., and Timasheff, S. N. (1986) *Biochemistry* **25**, 6214–6222
- Wang, Z., and Sheetz, M. P. (2000) *Biophys. J.* **78**, 1955–1964
- Liliom, K., Wagner, G., Pácz, A., Cascante, M., Kovács, J., and Ovádi, J. (2000) *Eur. J. Biochem.* **267**, 4731–4739
- Tracey, D. E., Lin, S. H., and Cebra, J. J. (1976) *Biochemistry* **15**, 624–629
- Pharmacia AB (1994) *BIATechnology Handbook*, Pharmacia Biosensor AB, Uppsala, Sweden
- Walsh, J. L., Keith, T. J., and Knull, H. R. (1989) *Biochim. Biophys. Acta* **999**, 64–70
- Volker, K. W., and Knull, H. R. (1993) *J. Mol. Rec.* **6**, 167–177
- Ottaway, J. H., and Mowbray, J. (1977) *Curr. Top. Cell Regul.* **12**, 107–208